

# NumeriKontrol: Adding Numeric Control to Diffusion Transformers for Instruction-based Image Editing

Zhenyu Xu  
East China Normal University

Xiaoqi Shen  
South China University of Technology

Haotian Nan  
East China Normal University

Xinyu Zhang  
East China Normal University

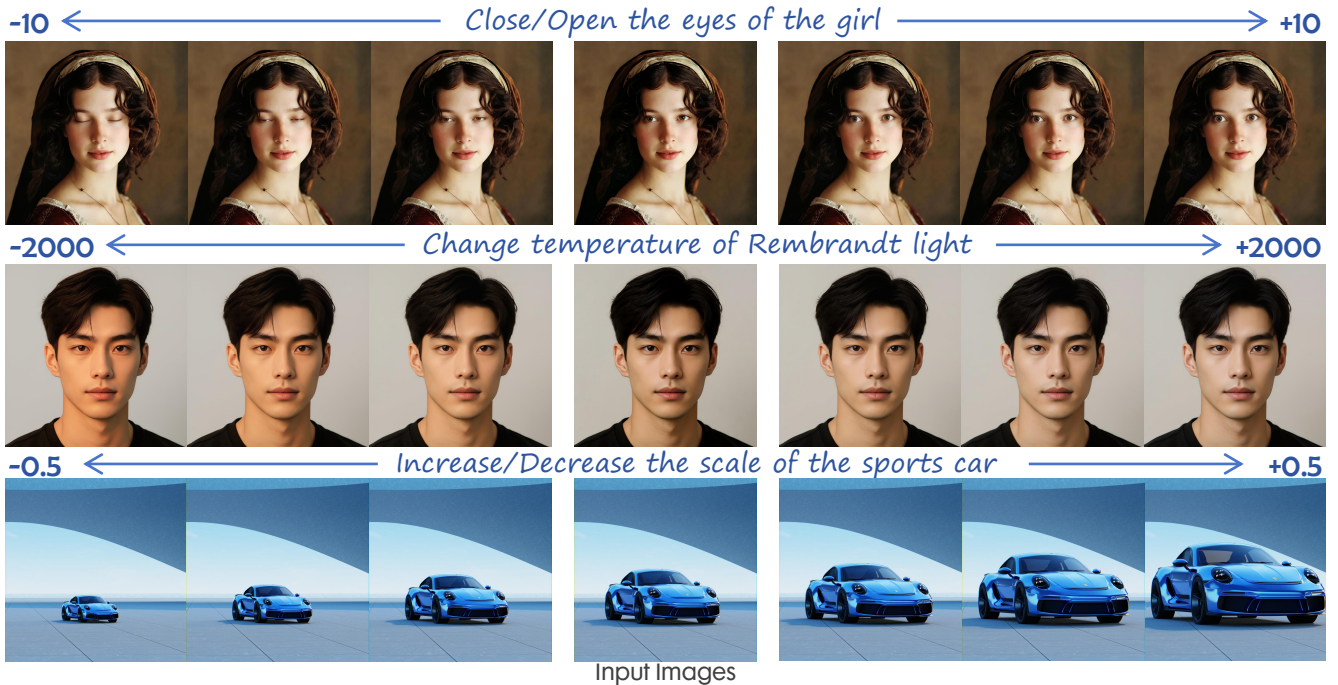


Figure 1. NumeriKontrol generates precise editing trajectories across diverse attributes conditioned on a source image, editing instruction, and numeric strength. Trained on our synthesized dataset, the model enables precise control over low-level and high-level editing tasks.

## Abstract

Instruction-based image editing enables intuitive manipulation through natural language commands. However, text instructions alone often lack the precision required for fine-grained control over edit intensity. We introduce NumeriKontrol, a framework that allows users to precisely adjust image attributes using continuous scalar values with common units. NumeriKontrol encodes numeric editing

scales via an effective Numeric Adapter and injects them into diffusion models in a plug-and-play manner. Thanks to a task-separated design, our approach supports zero-shot multi-condition editing, allowing users to specify multiple instructions in any order. To provide high-quality supervision, we synthesize precise training data from reliable sources, including high-fidelity rendering engines and DSLR cameras. Our Common Attribute Transform (CAT) dataset covers diverse attribute manipulations with accu-

rate ground-truth scales, enabling NumeriKontrol to function as a simple yet powerful interactive editing studio. Extensive experiments show that NumeriKontrol delivers accurate, continuous, and stable scale control across a wide range of attribute editing scenarios. These contributions advance instruction-based image editing by enabling precise, scalable, and user-controllable image manipulation.

## 1. Introduction

Recent advancements in text-to-image generative models [13, 38] have enabled instruction-driven image editing [2], allowing users to modify images via natural language instructions. However, effective editing requires controlling not only *what* to edit but also *how much*. For instance, designers may need to precisely adjust a character’s smile, while photographers may require fine-grained control over the light effect of the image (Fig. 1). This numeric precision in image editing remains largely underexplored, yet is crucial for bridging intuitive language interfaces with fine-grained parametric control.

Previous researches achieving fine-grained control via editing instructions mainly focus on continuous editing. Early GAN-based approaches [1, 10, 20, 32, 34] addressed the challenge through latent space manipulation for continuous attribute control. The effectiveness of these methods highly depend on the smoothness of latent space. Moreover, each GAN model should train from scratch. Other solutions based on diffusion models incorporating strength parameters [6, 41] have demonstrated effective material editing, but they only limit on specific domain. Kontinuous Kontext [33] extends this paradigm to a unified instruction-based editing framework across diverse scenarios. It takes advantage of the modulation space introduced in Diffusion Transformers (DiT). However, the reliance of Kontinuous Kontext on morphing-synthesized training data compromises numeric fidelity. Meanwhile, all of these methods edit the image with a normalized parameter ranging from 0 to 1. This ambiguates the actual effect of the instruction. More accurate instruction-based method is needed for better numeric controlled editing.

Despite the demand for the fine-grained editing, several obstacles are essential to step over. The basic requirement is to preserve the image consistency while only attributes in the image changes along the input number. Additionally, the nonlinearity of the text embedding space is a major problem, limiting the effectiveness of introducing numbers into the prompt directly. Simultaneously, the unit in various scenarios differs from each other. The same numbers from two dimensions presents absolutely differed visual effects on the same image. Of particular concern is that there is no previous dataset indexed with accurate attribute transitions. Previous approaches [2, 33] synthesize the dataset through

Large Language Models (LLM), or provide a domain specific dataset [6, 41].

In this paper, we present NumeriKontrol, an instruction-based editing model that enables explicit quantitative control through parametric specifications in text prompts with diverse units. Utilizing the editing priors that ensure object and character preservation of FLUX.1 Kontext [19], we introduce an effective numeric adapter. It encodes parametric values from prompts into embeddings, which are fused with task IDs for isolating different units. These numeric embeddings are as the same dimension as embeddings of instructions. The embeddings are injected into the DiT models by concatenating it to the text tokens. Benefit from such an In Context Learning (ICL) approach, NumeriKontrol support zero-shot multi-numeric instruction editing. As the units are separated, the model produces identical results however the order the instructions are. To train NumeriKontrol, we construct the Common Attribute Transformation (CAT) dataset, comprising fundamental editing scenarios with ground-truth numeric value annotated. Crucially, all edited images are sourced from rendering engines or camera captures rather than synthetic interpolations for LLM-generated, ensuring the model learns genuine correspondences between numerical parameters and their visual manifestations. Meanwhile, the whole image maintains consistency with only the attribute mentioned in the instruction modifying.

Our main contributions can be summarized as follows:

- We introduce the task of precise numeric control in instruction-based image editing while maintaining high consistency across the entire image.
- We propose a plug-and-play adapter for injecting numeric information into existing DiT models, enabling precise numeric control via an in-context learning paradigm.
- We synthesize a comprehensive dataset for common editing scenarios, covering general image editing operations with ground-truth control annotations. Extensive experiments across diverse editing tasks demonstrate that NumeriKontrol achieves superior precision and consistency compared to existing methods.

## 2. Related Works

### 2.1. Diffusion Models

Diffusion models have emerged as a prominent class of generative models, evolving from their foundational denoising probabilistic frameworks to state-of-the-art architectures [13, 38, 44]. These models have demonstrated remarkable efficacy across diverse image generation tasks, including text-to-image synthesis [36, 39] and image editing [2, 3, 17]. Through iterative noise refinement processes, diffusion models achieve unprecedented fidelity and diversity in generated content. Early latent diffusion mod-

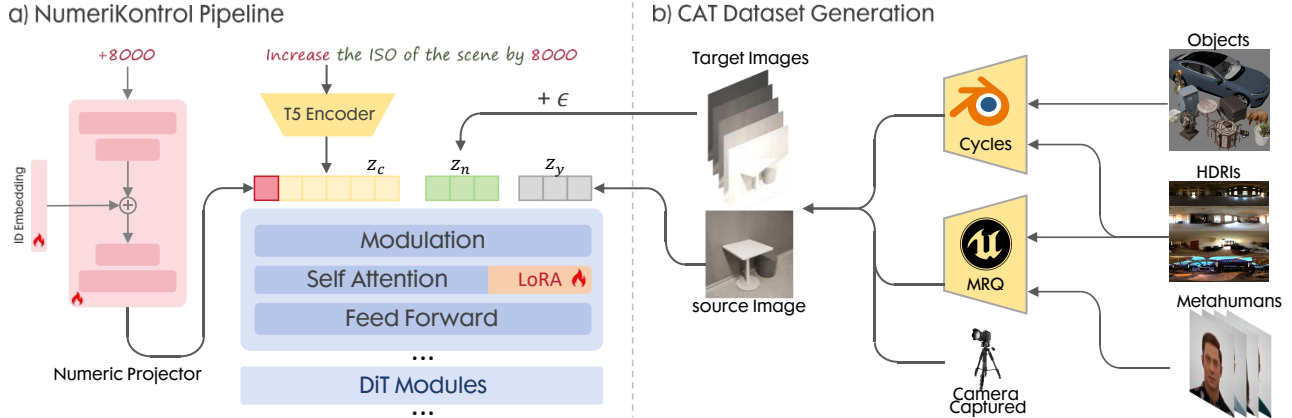


Figure 2. **a) Overall pipeline of NumeriKontrol.** Numeric information is extracted from the editing instruction and encoded, subsequently being fused with the task ID embedding. Positive and negative numeric editing operations share an identical task ID. We construct a comprehensive operation dataset comprising both synthetically generated and real-captured images. **b) Dataset generation.** Dataset diversity is ensured through heterogeneous data sources. During training, origin and context images are randomly sampled from the attribute animation sequences.

els (LDMs) leveraged CLIP [37] to align text and image representations within a shared latent space. Recently, a paradigm shift has occurred in diffusion model architectures, transitioning from conventional U-Net-based designs to transformer-based frameworks. This architectural evolution, exemplified by models such as SD3 [7] and FLUX [18], adopts Diffusion Transformer [35] structures that enable enhanced image quality, higher-resolution synthesis, and improved processing of complex conditional inputs. These transformer-based models modulate text tokens extracted from CLIP encoders with embeddings from language models and noised latent representations.

## 2.2. Controllable Generation

The synthesis process of diffusion models can be controlled across multiple dimensions. LoRA [14] enables fine-tuning of LDMs to generate images with desired characteristics. ControlNet [56] and subsequent works [5, 25–30, 45, 58, 60] leverages structural information by incorporating trainable copies of the diffusion model’s encoding layers to guide generation. T2I-Adapter [31] enhances computational efficiency through lightweight adapter modules. IP-Adapter [54] introduces disentangled cross-attention through an additional encoder to fit for non-aligned condition tasks. With the architectural transition to Diffusion Transformers [35], recent approaches such as EasyControl [59] and OmniControl [49] have achieved image-conditioned generation within MM-DiT frameworks and inspired subsequent works [8, 9, 16, 21, 42, 43, 46–48, 51]. However, existing research predominantly focuses on image-based guidance, leaving a gap in numerical control methods that would enable more precise and quantitative manipulation of generated content.

## 2.3. Instruction-based Image Editing

Instruction-based image editing, pioneered by Instruct-Pix2Pix [2], enables image manipulation through natural language instructions. To achieve this, the authors curated a large-scale synthetic dataset comprising image-edit pairs generated via Prompt2Prompt [11], with corresponding editing instructions synthesized by large language models (LLMs). More recent approaches [15, 23, 40, 52, 53] have developed unified large-scale models capable of performing both generation and editing tasks [22–24]. These models demonstrate proficiency across diverse editing operations, including subject-driven personalization, compositional scene editing, and instruction-guided modifications. Despite their impressive versatility in general-purpose editing scenarios, these models lack mechanisms for numerical control over editing attributes, thereby limiting their utility for applications requiring precise, fine-grained adjustments.

## 3. Preliminary

**Problem Formulation.** For instruction-based image editing, a model synthesizes an edited image following a reference image  $c$  and a text editing prompt  $y$ . It aims at learning the conditional distribution  $p(x | c, y)$ . We define our task by extending general instruction-based image editing with a numeric strength. For any editing instruction  $y$  containing an attribute value  $n$ , the model aims at approximating the conditional distribution  $p(x | c, y, n)$ . Approaching the distribution by diffusion model [7, 36, 38], the target is to obtain a network  $\epsilon_\theta(x(t), y, c, n)$  that predicting a noise. The result  $x$  can be obtained via several denoising steps.

**FLUX.1 Kontext.** FLUX [18] is a Text-to-Image model

build upon Diffusion Transformers. FLUX.1 Kontext [19] fine-tunes the FLUX model to fit in image editing tasks. It takes a source image and an edit instruction as input and outputs the edited result. In this pipeline, the image and text are encoded as tokens and processed through visual and textual attention streams. Kontext extends to editing tasks by encoding the source (context) image with the autoencoder. The context token is then concatenated to the noise tokens, which are jointly processed in the visual stream. As FLUX.1 Kontext achieves the network  $\epsilon_\theta(x(t), y, c)$ , the problem switches to how to inject  $n$  into the model.

## 4. Method

In this section, we propose a numeric projector to encode numeric strength and integrate it into the MM-DiT architecture (Sec. 4.1 and 4.2). For multi-condition scenarios, we introduce a decoupled attention masking strategy to prevent cross-condition interference (Sec. 4.3). Finally, we describe the dataset construction combining rendering engine-generated samples and camera-captured photographs (Sec. 4.4).

### 4.1. Unit Isolated Numeric Projector

Given that FLUX.1 Kontext provides a prior for image consistency, our objective is to inject numeric edit strength information into the Diffusion Transformers. Since numeric information is embedded within the instruction, we investigate whether fine-tuning on data with captions containing numbers suffices. Through empirical study, we fine-tune the FLUX.1 Kontext model and observe that direct learning of numeric transitions proves infeasible. Fine-tuning on such datasets results in the model generating averaged representations according to the prompts. Notably, numeric information is almost entirely discarded during the training process.

To address the limitation, we propose a lightweight numeric projector that explicitly encode strength information. This adapter encodes any strength value  $\bar{n}$  from instruction  $y$  into a feature representation  $z_{\bar{n}} \in \mathbb{R}^{1 \times d}$  via several MLP layers. The major concern lies in that two attributes to be edited may have different units but same values. Consider moving an object 10cm forward and rotating 10 degrees along the Z-axis. If the number is encoded into one token identically, the token undertakes representing two definitely different attribute. Consequently, the model may rotate the object by 10 degree while the user intends to move forward. We therefore design a two-stage process with task fusion. Initially, the strength value  $n$  is encoded into hidden states  $H_n$ . A trainable task-specific identifier  $\mathbf{T}$  is embedded and fused with  $H_n$  to accommodate diverse editing tasks. Subsequently, the hidden states are decoded through the MLP, yielding  $z_{\bar{n}}$ . The complete encoding process can be formu-

lated as:

$$z_{\bar{n}} = \mathcal{D}(\mathcal{E}(n) + \text{emb}(\mathbf{T})), \quad (1)$$

where  $\mathcal{E}$  and  $\mathcal{D}$  denote MLPs functioning as encoder and decoder, respectively. When several numbers with same value but different units are encountered, the task embeddings separate these tokens into their own dimensions. It effectively avoids task-switching during inference.

### 4.2. Numeric Adaptation into MM-DiT

Within the FLUX.1 Kontext architecture, the model processes three distinct types of input features: text tokens  $z_t$ , noise representations  $z_n$ , and context tokens  $z_y$ . These input features are initially projected into their respective query  $\mathbf{Q}$ , key  $\mathbf{K}$ , and value  $\mathbf{V}$  representations through learnable projection matrices, as formulated below:

$$\begin{aligned} \mathbf{Q}_t &= W_{\mathbf{Q}}z_t, \mathbf{K}_t = W_{\mathbf{K}}z_t, \mathbf{V}_t = W_{\mathbf{V}}z_t, \\ \mathbf{Q}_n &= W_{\mathbf{Q}}z_{ny}, \mathbf{K}_n = W_{\mathbf{K}}z_{ny}, \mathbf{V}_n = W_{\mathbf{V}}z_{ny}, \end{aligned} \quad (2)$$

where  $z_{ny} = [z_n, z_y]$  denotes the concatenation of noise and context tokens. Subsequently, these projected features are concatenated across modalities to form unified representations  $[\mathbf{Q}_t, \mathbf{Q}_n]$ ,  $[\mathbf{K}_t, \mathbf{K}_n]$ , and  $[\mathbf{V}_t, \mathbf{V}_n]$ , which are then processed through a self-attention, depicted in Fig. 2 (a).

To exploit the in-context learning capabilities of MM-DiT, we introduce a modified attention formulation. This formulation directly integrates numeric tokens  $\bar{n}$  into the text token stream. Concretely, we concatenate numeric token representations with text tokens prior to projection:

$$\mathbf{Q}_t = W_{\mathbf{Q}}[z_{\bar{n}}, z_t], \mathbf{K}_t = W_{\mathbf{K}}[z_{\bar{n}}, z_t], \mathbf{V}_t = W_{\mathbf{V}}[z_{\bar{n}}, z_t]. \quad (3)$$

Consequently, the original text query representation  $\mathbf{Q}_t$  in Eq. 3 is replaced by the extended representation  $[\mathbf{Q}_{\bar{n}}, \mathbf{Q}_t]$ , enabling the model to jointly attend to both numeric and textual information. To enable the DiT further understand the concatenation of the numeric token and text tokens, all  $W_{\mathbf{Q}}, W_{\mathbf{K}}$  and  $W_{\mathbf{V}}$  utilizes Low-rank Adaptations [14] during model training.

For model training, we construct a paired dataset comprising quadruplets of  $(x, c, n, y)$ , representing source image, editing instruction, numeric editing parameter and target edited image correspondingly. Given a training sample  $(x, y, c, n)$  and a randomly sampled diffusion timestep  $t$ , we optimize the model parameters using the standard flow matching objective:

$$\mathcal{L}_\theta = \mathbb{E}_{t \sim p(t), y, c, n} \|v_\theta(x^t, y, c, n, t) - (\epsilon - x)\|_2^2, \quad (4)$$

where  $x^t$  represents the interpolated latent representation between the clean latent  $y_c$  and Gaussian noise  $\epsilon \sim \mathcal{N}(0, 1)$ , computed as  $x^t = (1-t)x + t\epsilon$ . Here,  $v_\theta$  denotes the transformers in FLUX.1 Kontext parameterized by  $\theta$ .

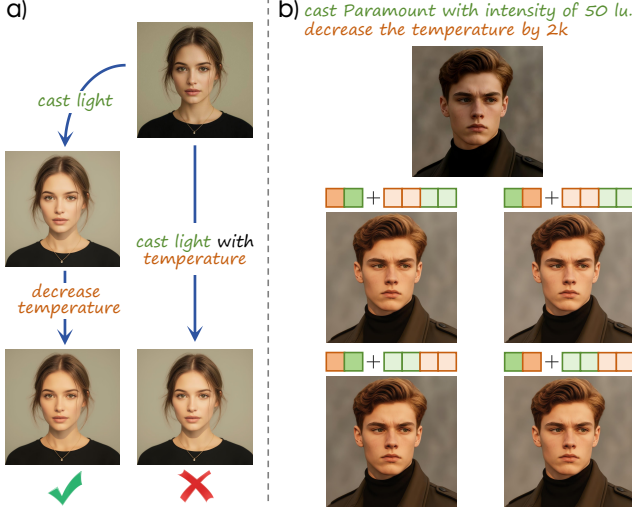


Figure 3. **a)** Example of resolving coupled instruction. Training directly on such instructions fails, as the real start point of the edit is the image casted by a light but not the source image. **b)** Visualization of decoupled and order-independent editing through multiple numeric instructions.

### 4.3. Decoupled Multi-numeric Editing

Generally, some editing tasks cannot be achieved by one attribute transformation, but can be decomposed into several simple tasks. For an instruction  $y$ , it may be actually separated into  $y_0, y_1, \dots, y_n$  to precisely describe the editing. As is shown in Fig. 3 (a), the instruction *Cast a light with temperature* should be resolved as *Cast a light with intensity of  $\|\bar{n}_0\|$  lumen* and *Change the temperature of the light by  $\|\bar{n}_1\|$  Kelvin*. Composed instructions make dataset construction and training more sophisticated, a multi-numeric editing is essential for such cases.

During training, each numeric token learns to interact with its corresponding task ID embedding, editing instruction template and context tokens. To enable multi-numeric conditioning, we develop a zero-shot multi-numeric paradigm inspired by EasyControl [59] in inference. For each sub-task, the numeric value is encoded as  $z_{\bar{n}_i}, i \in N$  where  $N$  represents number of tasks. All numeric tokens are concatenated as  $[z_{\bar{n}_0}, z_{\bar{n}_1}, \dots, z_{\bar{n}_N}]$ . Each task corresponds to an instruction template, the final instruction concatenated from all of the sub-instructions.

In multi-numeric inference, cross-attention between numeric tokens from different conditions introduces undesired interference. A structured attention mask is employed that isolates different numeric tokens while allowing noise tokens to aggregate information from all sources. For  $N$  numeric conditions, the self-attention sequence is constructed as:

$$\mathbf{Z} = [z_{\bar{n}_1}, z_{\bar{n}_2}, \dots, z_{\bar{n}_m}, z_t, z_n], \quad (5)$$

where  $z_{\bar{n}_i}, z_t$ , and  $z_n$  represent tokens for the  $i$ -th numeric condition, text tokens, and noise tokens, respectively. We define an attention mask  $M \in \{0, -\infty\}^{n \times n}$  as:

$$M_{ij} = \begin{cases} 0, & \text{if } (i, j \in \mathcal{I}_t \cup \mathcal{I}_n) \text{ or } (i = j). \\ -\infty, & \text{otherwise.} \end{cases} \quad (6)$$

where  $\mathcal{I}_t$  and  $\mathcal{I}_n$  denote the index sets of text and noise tokens. This masking ensures that numeric tokens from different conditions remain isolated while noise tokens attend to all conditions. It prevents mutual interference while preserving independent conditional control. During our experiment, we found that the order of the editing prompts and numeric tokens does not influence the result, illustrated in Fig. 3 (b). As the numeric tokens are fused by the task embeddings, it only interacts with corresponding text tokens. This phenomenon lies on the editing-consistency prior of FLUX Kontext. It tends to predict an origin image if the editing is not available or understood by the model.

### 4.4. Synthesize Attribute Dataset

A heuristic approach to achieve continuous editing control is to generate intermediate images by interpolating between the source and edited images. Existing diffusion-based morphing methods [4, 55] interpolate in the latent space, assuming semantic smoothness. However, this assumption does not hold universally. Such methods are sensitive to outliers and frequently produce artifacts in intermediate results, including missing objects and blurred content (Fig. 4). As depicted in Fig. 2 (b), we construct a dataset from two complementary sources to enable broader numeric control:

**Rendering Engine-Based Data Generation.** For editing operations difficult to capture in real-world settings, we re-

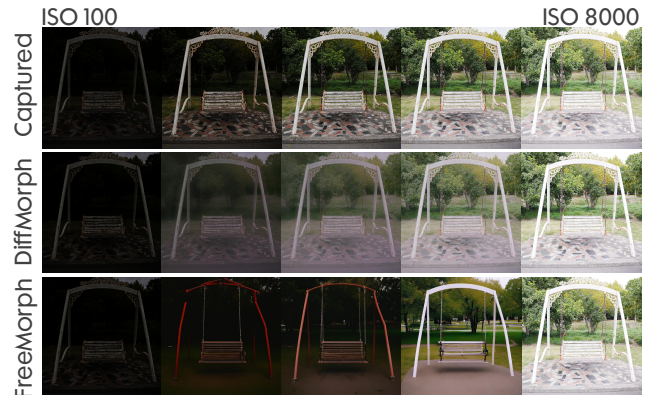


Figure 4. **Illustration of difference from physically synthesized data to morphing-generated intermediates.** Interpolation-based morphing methods fail to preserve visual fidelity even in straightforward low-level editing scenarios such as ISO modification. FreeMorph, a representative diffusion-based morphing technique, samples trajectories with substantial deviation from ground truth sequences.

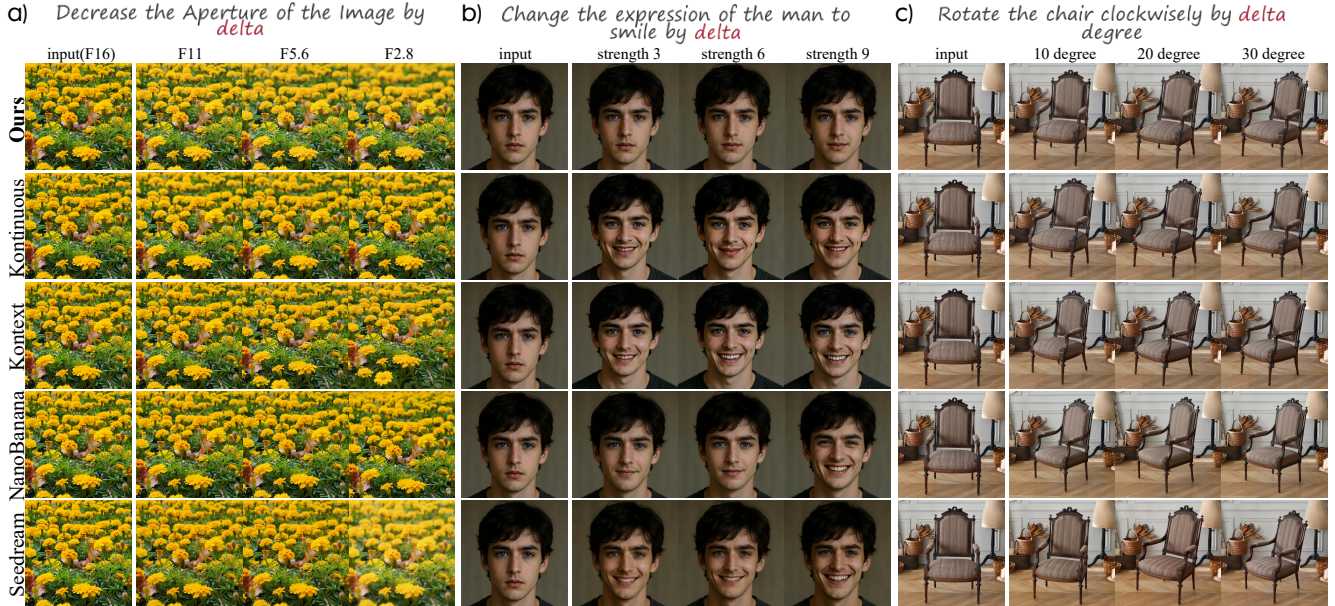


Figure 5. **Visualization results on NumeriKontrol and baseline methods.** Various scenarios, including outdoor scene, portrait and object editing, are selected from the results. The "delta" in each caption is replaced by the actual number above the images in NumeriKontrol. Captions of other methods are tuned respectively. Compared to others, the smile of the man generated by NumeriKontrol is less prominent because the model learned from a dataset containing only subtle smile examples.

fer to professional rendering engines, Blender and Unreal Engine, to generate physically plausible and visually realistic images. Cycles renderer and MRQ system with path tracing are used in these two engines respectively, ensuring high-quality render results. For object transformations, Blender is chosen to manipulate 3D assets. We collect a large amount of FBX objects and HDRI backgrounds online. Each scene comprises an object (ranging from small items to vehicles) and one of HDRI backgrounds. For example, we apply rotations ranging from  $-90$  degree to  $90$  degree, sampling 180 rotation states into dataset. For human face and pose animations, we employ the Unreal MetaHuman Editor to generate 100 distinct characters across various ages, each rendered in a different HDRI environments. Since scenarios as facial expressions and pose transition lack inherent numeric parameterization, we encode the origin status as 0 and map target expressions to  $\pm 10$ . The instruction of each scenario is human-designed for better understanding. For better generalization, the camera view point is selected randomly from the half-sphere centered at the object.

#### Camera-Captured Dataset. Camera-Captured Dataset.

Rendering engines excel at geometric transformations but fail to reproduce realistic camera-specific effects. To enable our model to function as a versatile camera studio, we capture real photographic data using a Digital Single-Lens Reflex (DSLR) camera. This provides authentic samples for camera parameter adjustments. For instance, we

collect 200 scenes with ISO values ranging from 100 to 8000 covering objects, indoor environments, and outdoor landscapes. Camera parameters typically exhibit nonlinear characteristics. We formulate the editing instruction as "Increase/Decrease the  $\mathbf{P}$  by  $\|\delta\|$ ", where  $\mathbf{P}$  denotes the target parameter and  $\delta$  represents the measured difference between source and target values. Other attributes are all captured in reasonable range. During training, the input and target image is randomly chosen and the  $\delta$  is calculated online for better generalization.

## 5. Experiments

### 5.1. Experiment Set Up

**Implementation Details.** We employed official FLUX.1 Kontext [19] pretrained model as the base model. The Numeric Projector is a four layer MLP with dimensions  $256 \rightarrow 256 \rightarrow 256 \rightarrow 4096$  in our experiments. The LoRA applied on attention layers of DiT is set to 128. During training, two A800 GPUs(80GB) are devoted into optimization progress, with a batch size of 4 per GPU, and a learning rate of  $5e-5$ , training over 160,000 steps. During inference, the flow-matching sampling is applied with 28 sampling steps.

**Baseline Methods.** We validate our method against several state-of-the-art methods. We choose FLUX.1 Kontext [19], Kontinuous Kontext [33], Nano Banana and Seedream 4.0 [40] as our baseline. The classifier-free guid-

Table 1. **Quantitative Comparison.** The best of each metric is **emphasized**.

Method	Low Level Tasks				High Level Tasks			
	PSNR $\uparrow$	SSIM $\uparrow$	MSE $\downarrow$	LPIPS $\downarrow$	PSNR $\uparrow$	SSIM $\uparrow$	MSE $\downarrow$	LPIPS $\downarrow$
FLUX.1 Kontext [19]	19.694	0.7169	0.0236	0.1264	18.214	0.7642	0.0289	0.1876
Kontinuous Kontext [33]	21.452	0.7366	0.0225	0.1079	24.753	0.8624	0.0117	0.0755
Nano Banana	18.272	0.5880	0.0413	0.2080	22.868	0.8688	0.0153	0.0984
Seedream [40]	13.659	0.5337	0.0721	0.3048	17.873	0.8202	0.0279	0.1411
<b>NumeriKontrol(Ours)</b>	<b>22.678</b>	<b>0.7633</b>	<b>0.0190</b>	<b>0.0980</b>	<b>27.560</b>	<b>0.9120</b>	<b>0.0084</b>	<b>0.0541</b>

ance [12] of FLUX.1 Kontext is set to 1.0. For Nano Banana and Seedream, official API and website is used in evaluation. As Kontinuous Kontext is not open-sourced, we implement it as is described in its paper. The models for Kontinuous are trained from a simpler CAT dataset, which removes the strength information from prompt and normalizes the parameters from 0 to 1.

**Benchmarks.** We construct a test set for the CAT dataset, comprising representative examples across fundamental editing scenarios. Based on task complexity, two evaluation categories are established. The first category encompasses low-level editing tasks that applied globally to the image, specifically adjustments as ISO sensitivity, aperture settings, white balance parameters and so on. The second category consists of high-level editing tasks that require spatial and semantic understanding, including facial expression manipulation, pose modification and other object-level operations. For diversity, an aspect of the dataset enable bidirectional manipulation as examples shown in Fig. 1. At last, totally 200 editing cases are included in the test set.

**Metrics.** To evaluate the quality and accuracy of results, we test the results on PSNR, SSIM [50], LPIPS [57] and Pixelwise Mean Square Loss (MSE). All metrics focus on the similarity and consistency against the ground truth.

## 5.2. Qualitative Comparison

We conduct qualitative comparisons between NumeriKontrol and baseline methods including Kontext [19], Kontinuous Kontext, Nano Banana and Seedream [40] to illustrate the effectiveness of NumeriKontrol. Three visual results covers different scenarios, including both low-level and high-level tasks. The results are shown in Fig. 5.

For aperture editing tasks shown in Fig. 5 (a), both LLM-based methods (Nano Banana and Seedream) fail to generate the desired effects, demonstrating inadequate understanding of the *Aperture* concept. Alternatively, These methods approximate similar results via similar instructions as *blur the farther flowers.*, but the resulting images remain substantially suboptimal. FLUX.1 Kontext also lacks comprehension of aperture semantics; nevertheless, it preserves the original image rather than introducing erroneous modifications. In contrast, NumeriKontrol and Kontinuous Kon-

text demonstrate competency in aperture manipulation due to their training on CAT. However, our method achieves superior aperture-matching performance. A notable limitation of Kontinuous is need for strength normalization. It is incompatible with non-linear design of camera F-numbers.

As illustrated in Fig. 5 (b) and (c), all methods successfully execute edits in accordance with user prompts for high-level tasks. However, FLUX.1 Kontext fails to preserve numeric information from the instructions, generating identical images regardless of attribute modifications. When provided with prompts such as *Change the expression of the man to smile by 0.3 strength. Full strength is 1.0*, Nano Banana and Seedream produce varied editing outcomes; the visual manifestations in the edited images do not exhibit a monotonic correspondence with user-specified strength values. Despite Kontinuous being trained on the same CAT dataset, its results deviate substantially from the ground truth.

## 5.3. Quantitative Comparison

We present quantitative comparisons with baseline methods in Table. 1 for further validating the accuracy of our approach. Low-level tasks operate primarily in the pixel domain, applying global adjustments without altering image content, whereas high-level tasks modify localized regions and introduce semantic-level changes. Given the fundamental distinctions between these task categories, metrics are computed separately for each.

Quantitative comparisons demonstrate that NumeriKontrol achieves superior performance on both low-level and high-level tasks, validating the generalization capability of our method in unseen scenarios. LLM-based methods, including Seedream and Nano Banana, exhibit stronger performance on high-level tasks compared to low-level tasks, which stems from their semantic understanding of input images and instruction comprehension. Conversely, FLUX.1 Kontext achieves higher scores on low-level tasks, which we attribute to Kontext’s robust prior for preserving overall image structure. Kontinuous fails to follow precise instructions, but keeps a coarse track on number sequences.

Table 2. **Quantitative results of the ablative study.** The best of each metric is **emphasized**. Line 1-4 sequentially decreases the LoRA while line 5-7 sequentially removes the module from model. Two series of experiments are evaluated separately.

Methods	PSNR $\uparrow$	SSIM $\uparrow$	MSE $\downarrow$	LPIPS $\downarrow$
<b>NumeriKontrol</b>	<b>25.119</b>	<b>0.8377</b>	<b>0.0137</b>	<b>0.0760</b>
LoRA Rank 64	22.766	0.8004	0.0182	0.0898
LoRA Rank 32	21.080	0.7903	0.0206	0.1020
LoRA Rank 4	20.263	0.7691	0.0235	0.1399
LoRA Rank 0	19.671	0.7524	0.0249	0.1553
w/o ID fusing	23.559	0.8065	0.0183	0.0721
w/o Projector	21.840	0.7447	0.0216	0.1258
w/o LoRA	18.953	0.7406	0.0262	0.1570

## 5.4. Ablative Study

To comprehensively evaluate the importance of each module in NumeriKontrol, we conduct ablation studies on our method. Quantitative results are presented in Table 2. We first preserve the Numeric Projector and progressively reduce the rank of LoRA introduced in Sec. 4.2. As the rank decreases, the trained model gradually loses the correspondence between numeric values and actual visual effects, as shown in Fig. 6 (a). When LoRA is completely removed, the model’s performance nearly degrades to that of standard FLUX.1 Kontext. When the rank decreases to 4, the model converges to only 1-2 cases per instruction template, demonstrating insufficient capacity for numeric control.

For the next ablation, we preserve the LoRA module and remove the task ID embedding from the Numeric Projector. This operation significantly impacts the MSE metric. As illustrated in Fig. 6(b), the generated images are influenced by unrelated attribute edits present in the dataset. We further remove the Numeric Projector entirely, retaining only the LoRA modules. In this configuration, the model learns limited representations of numeric information and fails to associate instructions with the desired visual effects for specific attribute values. Visual results are shown in Fig. 6 (c).

## 5.5. Failure Cases

NumeriKontrol exhibits limitations in certain tasks. For translation operations, we encode the displacement  $e_x, e_y, e_z$  into tokens  $z_e \in \mathbb{R}^{3 \times 4096}$  and concatenate them with the instruction *Translate the object by*  $(e_x, e_y, e_z)$ . We apply a similar approach to Euler angle rotations. Our method fails to establish a clear correspondence between the specified movements and the resulting images as demonstrated in Fig. 7 (a). Additional cases occur in scenarios with complex lighting conditions, as shown in Fig. 7 (b).

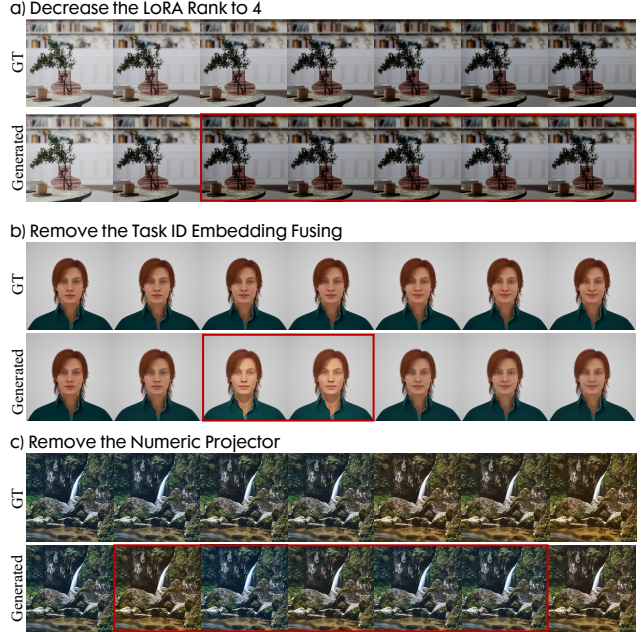


Figure 6. **Visualization of ablative study.** a) Gamma adjustment from 1.0 to 3.0. b) Without task embedding, cross-attribute interference occurs due to overlapping value ranges. c) Adjust the color hue. The relationship between generated images and ground truth (GT) is disordered without Numeric Projector.

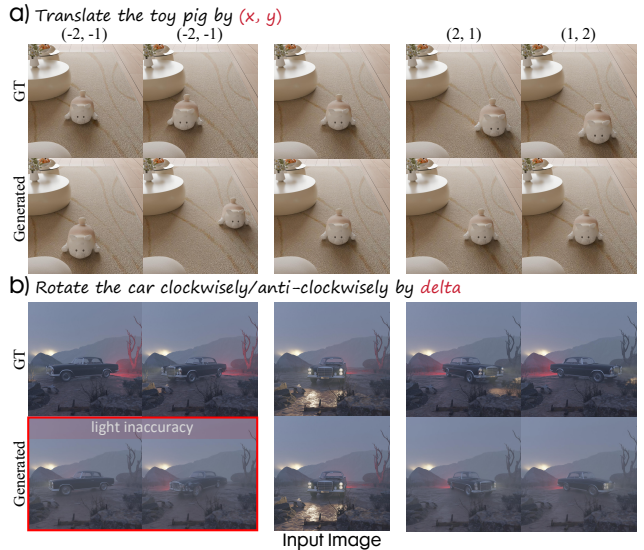


Figure 7. **Visualization of Failure cases.** a) Multi-numeric editing fails to translate an object by the specified vector. b) NumeriKontrol fails to preserve the lighting of the car.

## 6. Conclusion

We present NumeriKontrol, a method that introduces precise numeric control into instruction-based editing. This work makes four key contributions. 1) To our

knowledge, we are the first to enable instruction-based image editing with explicit numeric parameters. **2)** We design a lightweight Numeric Adapter to effectively encode parameters with different units. The numeric token integrates into the diffusion model in a plug-and-play manner. **3)** We propose a multi-numeric editing paradigm that handles combined instructions. **4)** We synthesize a large Common Attribute Transformation dataset with physically-accurate content. Each sample is annotated with edited attribute types and scales. This dataset serves as a training resource for NumeriKontrol and benefits the broader research community on similar tasks. Comprehensive experiments demonstrate that NumeriKontrol outperforms state-of-the-art models on numeric-specified editing tasks. Future research will broaden the applicability to more complex editing tasks.

## References

- [1] Rameen Abdal, Peihao Zhu, Niloy J Mitra, and Peter Wonka. Styleflow: Attribute-conditioned exploration of stylegan-generated images using conditional continuous normalizing flows. *ACM Transactions on Graphics*, 40(3):1–21, 2021. 2
- [2] Tim Brooks, Aleksander Holynski, and Alexei A Efros. Instructpix2pix: Learning to follow image editing instructions. In *Proceedings of the IEEE/CVF conference on computer vision and pattern recognition*, pages 18392–18402, 2023. 2, 3
- [3] Mingdeng Cao, Xintao Wang, Zhongang Qi, Ying Shan, Xiaoohu Qie, and Yinqiang Zheng. Masactrl: Tuning-free mutual self-attention control for consistent image synthesis and editing. In *Proceedings of the IEEE/CVF international conference on computer vision*, pages 22560–22570, 2023. 2
- [4] Yukang Cao, Chenyang Si, Jinghao Wang, and Ziwei Liu. Freemorph: Tuning-free generalized image morphing with diffusion model. *arXiv preprint arXiv:2507.01953*, 2025. 5
- [5] Xuewei Chen, Zhimin Chen, and Yiren Song. Transanimate: Taming layer diffusion to generate rgba video. *arXiv preprint arXiv:2503.17934*, 2025. 3
- [6] Ta Ying Cheng, Prafull Sharma, Mark Boss, and Varun Jampani. Marble: Material recomposition and blending in clip-space. In *Proceedings of the Computer Vision and Pattern Recognition Conference*, pages 13061–13071, 2025. 2
- [7] Patrick Esser, Sumith Kulal, Andreas Blattmann, Rahim Entezari, Jonas Müller, Harry Saini, Yam Levi, Dominik Lorenz, Axel Sauer, Frederic Boesel, et al. Scaling rectified flow transformers for high-resolution image synthesis. In *Forty-first international conference on machine learning*, 2024. 3
- [8] Yan Gong, Yiren Song, Yicheng Li, Chenglin Li, and Yin Zhang. Relationadapter: Learning and transferring visual relation with diffusion transformers. *arXiv preprint arXiv:2506.02528*, 2025. 3
- [9] Hailong Guo, Bohan Zeng, Yiren Song, Wentao Zhang, Chuang Zhang, and Jiaming Liu. Any2anytryon: Leveraging adaptive position embeddings for versatile virtual clothing tasks. *arXiv preprint arXiv:2501.15891*, 2025. 3
- [10] Erik Härkönen, Aaron Hertzmann, Jaakko Lehtinen, and Sylvain Paris. Ganspace: discovering interpretable gan controls. In *Proceedings of the 34th International Conference on Neural Information Processing Systems*, Red Hook, NY, USA, 2020. Curran Associates Inc. 2
- [11] Amir Hertz, Ron Mokady, Jay Tenenbaum, Kfir Aberman, Yael Pritch, and Daniel Cohen-Or. Prompt-to-prompt image editing with cross attention control. *arXiv preprint arXiv:2208.01626*, 2022. 3
- [12] Jonathan Ho and Tim Salimans. Classifier-free diffusion guidance. *arXiv preprint arXiv:2207.12598*, 2022. 7
- [13] Jonathan Ho, Ajay Jain, and Pieter Abbeel. Denoising diffusion probabilistic models. In *Proceedings of the 34th International Conference on Neural Information Processing Systems*, Red Hook, NY, USA, 2020. Curran Associates Inc. 2
- [14] Edward J Hu, Yelong Shen, Phillip Wallis, Zeyuan Allen-Zhu, Yuanzhi Li, Shean Wang, Lu Wang, Weizhu Chen, et al. Lora: Low-rank adaptation of large language models. In *The Tenth International Conference on Learning Representations*, page 3, 2022. 3, 4
- [15] Shijie Huang, Yiren Song, Yuxuan Zhang, Hailong Guo, Xueyin Wang, Mike Zheng Shou, and Jiaming Liu. Photodoodle: Learning artistic image editing from few-shot pairwise data. *arXiv preprint arXiv:2502.14397*, 2025. 3
- [16] Yuxin Jiang, Yuchao Gu, Yiren Song, Ivor Tsang, and Mike Zheng Shou. Personalized vision via visual in-context learning. *arXiv preprint arXiv:2509.25172*, 2025. 3
- [17] Bahjat Kawar, Shiran Zada, Oran Lang, Omer Tov, Huiwen Chang, Tali Dekel, Inbar Mosseri, and Michal Irani. Imagic: Text-based real image editing with diffusion models. In *Proceedings of the IEEE/CVF conference on computer vision and pattern recognition*, pages 6007–6017, 2023. 2
- [18] Black Forest Labs. Flux. <https://github.com/black-forest-labs/flux>, 2024. 3
- [19] Black Forest Labs, Stephen Batifol, Andreas Blattmann, Frederic Boesel, Saksham Consul, Cyril Diagne, Tim Dockhorn, Jack English, Zion English, Patrick Esser, et al. Flux. 1 kontext: Flow matching for in-context image generation and editing in latent space. *arXiv preprint arXiv:2506.15742*, 2025. 2, 4, 6, 7, 1
- [20] Xiaoming Li, Xinyu Hou, and Chen Change Loy. When stylegan meets stable diffusion: a w+ adapter for personalized image generation. In *Proceedings of the IEEE/CVF Conference on Computer Vision and Pattern Recognition*, pages 2187–2196, 2024. 2
- [21] Runnan Lu, Yuxuan Zhang, Jiaming Liu, Haofan Wang, and Yiren Song. Easytext: Controllable diffusion transformer for multilingual text rendering. *arXiv preprint arXiv:2505.24417*, 2025. 3
- [22] Yue Ma, Yali Wang, Yue Wu, Ziyu Lyu, Siran Chen, Xiu Li, and Yu Qiao. Visual knowledge graph for human action reasoning in videos. In *Proceedings of the 30th ACM International Conference on Multimedia*, pages 4132–4141, 2022. 3
- [23] Yue Ma, Xiaodong Cun, Yingqing He, Chenyang Qi, Xintao Wang, Ying Shan, Xiu Li, and Qifeng Chen. Magicstick: Controllable video editing via control handle transformations. *arXiv preprint arXiv:2312.03047*, 2023. 3

- [24] Yue Ma, Yingqing He, Xiaodong Cun, Xintao Wang, Siran Chen, Xiu Li, and Qifeng Chen. Follow your pose: Pose-guided text-to-video generation using pose-free videos. In *Proceedings of the AAAI Conference on Artificial Intelligence*, pages 4117–4125, 2024. 3
- [25] Yue Ma, Hongyu Liu, Hongfa Wang, Heng Pan, Yingqing He, Junkun Yuan, Ailing Zeng, Chengfei Cai, Heung-Yeung Shum, Wei Liu, et al. Follow-your-emoji: Fine-controllable and expressive freestyle portrait animation. In *SIGGRAPH Asia 2024 Conference Papers*, pages 1–12, 2024. 3
- [26] Yue Ma, Kunyu Feng, Zhongyuan Hu, Xinyu Wang, Yucheng Wang, Mingzhe Zheng, Xuanhua He, Chenyang Zhu, Hongyu Liu, Yingqing He, et al. Controllable video generation: A survey. *arXiv preprint arXiv:2507.16869*, 2025.
- [27] Yue Ma, Kunyu Feng, Xinhua Zhang, Hongyu Liu, David Junhao Zhang, Jinbo Xing, Yinhan Zhang, Ayden Yang, Zeyu Wang, and Qifeng Chen. Follow-your-creation: Empowering 4d creation through video inpainting. *arXiv preprint arXiv:2506.04590*, 2025.
- [28] Yue Ma, Yingqing He, Hongfa Wang, Andong Wang, Leqi Shen, Chenyang Qi, Jixuan Ying, Chengfei Cai, Zhifeng Li, Heung-Yeung Shum, et al. Follow-your-click: Open-domain regional image animation via motion prompts. In *Proceedings of the AAAI Conference on Artificial Intelligence*, pages 6018–6026, 2025.
- [29] Yue Ma, Yulong Liu, Qiyuan Zhu, Ayden Yang, Kunyu Feng, Xinhua Zhang, Zhifeng Li, Sirui Han, Chenyang Qi, and Qifeng Chen. Follow-your-motion: Video motion transfer via efficient spatial-temporal decoupled finetuning. *arXiv preprint arXiv:2506.05207*, 2025.
- [30] Yue Ma, Zexuan Yan, Hongyu Liu, Hongfa Wang, Heng Pan, Yingqing He, Junkun Yuan, Ailing Zeng, Chengfei Cai, Heung-Yeung Shum, et al. Follow-your-emoji-faster: Towards efficient, fine-controllable, and expressive freestyle portrait animation. *arXiv preprint arXiv:2509.16630*, 2025. 3
- [31] Chong Mou, Xintao Wang, Liangbin Xie, Yanze Wu, Jian Zhang, Zhongang Qi, and Ying Shan. T2i-adapter: learning adapters to dig out more controllable ability for text-to-image diffusion models. In *Proceedings of the Thirty-Eighth AAAI Conference on Artificial Intelligence and Thirty-Sixth Conference on Innovative Applications of Artificial Intelligence and Fourteenth Symposium on Educational Advances in Artificial Intelligence*. AAAI Press, 2024. 3
- [32] Rishubh Parihar, VS Sachidanand, Sabariswaran Mani, Tejan Karmali, and R Venkatesh Babu. Precisecontrol: Enhancing text-to-image diffusion models with fine-grained attribute control. In *European Conference on Computer Vision*, pages 469–487. Springer, 2024. 2
- [33] Rishubh Parihar, Or Patashnik, Daniil Ostashev, R Venkatesh Babu, Daniel Cohen-Or, and Kuan-Chieh Wang. Kontinuous kontext: Continuous strength control for instruction-based image editing. *arXiv preprint arXiv:2510.08532*, 2025. 2, 6, 7, 1
- [34] Or Patashnik, Zongze Wu, Eli Shechtman, Daniel Cohen-Or, and Dani Lischinski. Styleclip: Text-driven manipulation of stylegan imagery. In *Proceedings of the IEEE/CVF international conference on computer vision*, pages 2085–2094, 2021. 2
- [35] William Peebles and Saining Xie. Scalable diffusion models with transformers. In *Proceedings of the IEEE/CVF international conference on computer vision*, pages 4195–4205, 2023. 3
- [36] Dustin Podell, Zion English, Kyle Lacey, Andreas Blattmann, Tim Dockhorn, Jonas Müller, Joe Penna, and Robin Rombach. Sdxl: Improving latent diffusion models for high-resolution image synthesis. *arXiv preprint arXiv:2307.01952*, 2023. 2, 3
- [37] Alec Radford, Jong Wook Kim, Chris Hallacy, Aditya Ramesh, Gabriel Goh, Sandhini Agarwal, Girish Sastry, Amanda Askell, Pamela Mishkin, Jack Clark, et al. Learning transferable visual models from natural language supervision. In *Proceedings of the 38th International Conference on Machine Learning*, pages 8748–8763. PmlR, 2021. 3
- [38] Robin Rombach, Andreas Blattmann, Dominik Lorenz, Patrick Esser, and Björn Ommer. High-resolution image synthesis with latent diffusion models. In *Proceedings of the IEEE/CVF conference on computer vision and pattern recognition*, pages 10684–10695, 2022. 2, 3
- [39] Chitwan Saharia, William Chan, Saurabh Saxena, Lala Lit, Jay Whang, Emily Denton, Seyed Kamyar Seyed Ghasemipour, Burcu Karagol Ayan, S. Sara Mahdavi, Raphael Gontijo-Lopes, Tim Salimans, Jonathan Ho, David J Fleet, and Mohammad Norouzi. Photorealistic text-to-image diffusion models with deep language understanding. In *Proceedings of the 36th International Conference on Neural Information Processing Systems*, Red Hook, NY, USA, 2022. Curran Associates Inc. 2
- [40] Team Seedream, Yunpeng Chen, Yu Gao, Lixue Gong, Meng Guo, Qiushan Guo, Zhiyao Guo, Xiaoxia Hou, Weilin Huang, Yixuan Huang, et al. Seedream 4.0: Toward next-generation multimodal image generation. *arXiv preprint arXiv:2509.20427*, 2025. 3, 6, 7, 1
- [41] Prafull Sharma, Varun Jampani, Yuanzhen Li, Xuhui Jia, Dmitry Lagun, Fredo Durand, Bill Freeman, and Mark Matthews. Alchemist: Parametric control of material properties with diffusion models. In *Proceedings of the IEEE/CVF Conference on Computer Vision and Pattern Recognition*, pages 24130–24141, 2024. 2
- [42] Wenda Shi, Yiren Song, Dengming Zhang, Jiaming Liu, and Xingxing Zou. Fonts: Text rendering with typography and style controls. *arXiv preprint arXiv:2412.00136*, 2024. 3
- [43] Wenda Shi, Yiren Song, Zihan Rao, Dengming Zhang, Jiaming Liu, and Xingxing Zou. Wordcon: Word-level typography control in scene text rendering. *arXiv preprint arXiv:2506.21276*, 2025. 3
- [44] Jiaming Song, Chenlin Meng, and Stefano Ermon. Denoising diffusion implicit models. In *9th International Conference on Learning Representations, ICLR 2021, Virtual Event, Austria, May 3-7, 2021*. OpenReview.net, 2021. 2
- [45] Yiren Song, Shijie Huang, Chen Yao, Xiaojun Ye, Hai Ci, Jiaming Liu, Yuxuan Zhang, and Mike Zheng Shou. Processpainter: Learn painting process from sequence data. *arXiv preprint arXiv:2406.06062*, 2024. 3

- [46] Yiren Song, Danze Chen, and Mike Zheng Shou. Layer-tracer: Cognitive-aligned layered svg synthesis via diffusion transformer. *arXiv preprint arXiv:2502.01105*, 2025. 3
- [47] Yiren Song, Cheng Liu, and Mike Zheng Shou. Makeanything: Harnessing diffusion transformers for multi-domain procedural sequence generation. *arXiv preprint arXiv:2502.01572*, 2025.
- [48] Yiren Song, Cheng Liu, and Mike Zheng Shou. Omniconsistency: Learning style-agnostic consistency from paired stylization data. *arXiv preprint arXiv:2505.18445*, 2025. 3
- [49] Zhenxiong Tan, Songhua Liu, Xingyi Yang, Qiaochu Xue, and Xinchao Wang. Ominicontrol: Minimal and universal control for diffusion transformer. In *Proceedings of the IEEE/CVF International Conference on Computer Vision*, pages 14940–14950, 2025. 3
- [50] Zhou Wang, A.C. Bovik, H.R. Sheikh, and E.P. Simoncelli. Image quality assessment: from error visibility to structural similarity. *IEEE Transactions on Image Processing*, 13(4): 600–612, 2004. 7
- [51] Zitong Wang, Hang Zhao, Qianyu Zhou, Xuequan Lu, Xi-angtai Li, and Yiren Song. Diffdecompose: Layer-wise decomposition of alpha-composited images via diffusion transformers. *arXiv preprint arXiv:2505.21541*, 2025. 3
- [52] Chenfei Wu, Jiahao Li, Jingren Zhou, Junyang Lin, Kaiyuan Gao, Kun Yan, Sheng-ming Yin, Shuai Bai, Xiao Xu, Yilei Chen, et al. Qwen-image technical report. *arXiv preprint arXiv:2508.02324*, 2025. 3
- [53] Chenyuan Wu, Pengfei Zheng, Ruiran Yan, Shitao Xiao, Xin Luo, Yueze Wang, Wanli Li, Xiyan Jiang, Yexin Liu, Junjie Zhou, et al. Omnigen2: Exploration to advanced multimodal generation. *arXiv preprint arXiv:2506.18871*, 2025. 3
- [54] Hu Ye, Jun Zhang, Sibao Liu, Xiao Han, and Wei Yang. Ip-adapter: Text compatible image prompt adapter for text-to-image diffusion models. *arXiv preprint arXiv:2308.06721*, 2023. 3
- [55] Kaiwen Zhang, Yifan Zhou, Xudong Xu, Bo Dai, and Xingang Pan. Diffmorpher: Unleashing the capability of diffusion models for image morphing. In *Proceedings of the IEEE/CVF Conference on Computer Vision and Pattern Recognition*, pages 7912–7921, 2024. 5
- [56] Lvmin Zhang, Anyi Rao, and Maneesh Agrawala. Adding conditional control to text-to-image diffusion models. In *Proceedings of the IEEE/CVF international conference on computer vision*, pages 3836–3847, 2023. 3
- [57] Richard Zhang, Phillip Isola, Alexei A Efros, Eli Shechtman, and Oliver Wang. The unreasonable effectiveness of deep features as a perceptual metric. In *Proceedings of the IEEE conference on computer vision and pattern recognition*, pages 586–595, 2018. 7
- [58] Yuxuan Zhang, Lifu Wei, Qing Zhang, Yiren Song, Jiaming Liu, Huaxia Li, Xu Tang, Yao Hu, and Haibo Zhao. Stablemakeup: When real-world makeup transfer meets diffusion model. *arXiv preprint arXiv:2403.07764*, 2024. 3
- [59] Yuxuan Zhang, Yirui Yuan, Yiren Song, Haofan Wang, and Jiaming Liu. Easycontrol: Adding efficient and flexible control for diffusion transformer. In *Proceedings of the IEEE/CVF International Conference on Computer Vision*, pages 19513–19524, 2025. 3, 5
- [60] Yuxuan Zhang, Qing Zhang, Yiren Song, Jichao Zhang, Hao Tang, and Jiaming Liu. Stable-hair: Real-world hair transfer via diffusion model. In *Proceedings of the AAAI Conference on Artificial Intelligence*, pages 10348–10356, 2025. 3

# NumeriKontrol: Adding Numeric Control to Diffusion Transformers for Instruction-based Image Editing

## Supplementary Material

### A. User Study

To further demonstrate the effectiveness of NumeriKontrol, we conduct a user study comparing five methods: NumeriKontrol, Kontinuous [33], FLUX.1 Kontext [19], Nano Banana, and Seedream 4.0 [40]. We sample 30 examples for each method. As described in Sec. 5.2, Nano Banana and Seedream do not support specific numerical instructions. All instructions are adjusted and tested to ensure consistent evaluation across methods.

Following standardized evaluation protocols, we anonymize all samples by removing method identifiers and randomize their presentation order. The study is conducted through an online questionnaire distributed to participants. Participants view examples from all five methods and rate each sample on a 1-5 Likert scale (allowing one decimal place). The evaluation includes three criteria: (1) *Is the image edited according to the instruction?* (2) *Does the edited result match the numeric information in the instruction?* (3) *How much do you prefer the edited result?* These questions correspond to success rate, numerical alignment, and user preference, respectively.

Table 3. User study with state-of-the-art methods. The best score is **emphasized**.

Method	Success ( $\uparrow$ )	Alignment ( $\uparrow$ )	Preference ( $\uparrow$ )
FLUX.1 Kontext [19]	3.64	2.70	3.57
Kontinuous Kontext [33]	4.75	4.24	3.85
Nano Banana	4.42	3.25	3.62
Seedream [40]	4.31	3.09	3.78
NumeriKontrol(Ours)	<b>4.80</b>	<b>4.57</b>	<b>4.08</b>

The results of the user study is shown in Tab. 3. Our method scores best in all three criteria.

### B. More Details for Comparison

#### B.1. Implementation Details for Comparison

As Kontinuous Kontext [33] is implemented by ourselves, the strength projector in our implementation is designed with dimensions of  $1536 \rightarrow 256 \rightarrow 128 \rightarrow 6144$ . The scale and shift are separated into 3072 dimensions respectively from the output of the projector. The modulation parameter is set to 1.0 in our experiments.

#### B.2. Quantitative Comparison

Certain prompts may not function properly with Nano Banana and Seedream. To address this limitation, we develop



Figure 8. The low-level task of editing the white balance of the image. The white balance is divided into 400 steps, with 200 lower and 200 higher.

adapted instruction formats for these methods. For camera-related aspects in the test set, we append "Work as a DSLR camera" to the instructions to enable editing. For other numeric instructions, we adopt the following format: "Edit the image with a strength of  $\delta$ . The full strength is  $\Delta$ , where  $\delta$  represents the current editing strength and  $\Delta$  denotes the maximum strength. Details of the numeric instructions are provided in Sec. 4.4. All instructions used in quantitative comparisons are standardized using these two approaches to ensure fair evaluation.

As described in Sec.5.3, LLM-based methods successfully edit images for low-level tasks. However, they fail to preserve accurate numeric information from the instructions. Consequently, these two methods perform poorly on low-level tasks. An example from the quantitative results is shown in Fig.8.

### C. Additional Results

Our method supports continuous editing through the online delta calculation described in Sec.4.2. However, errors may accumulate during successive operations. As illustrated in

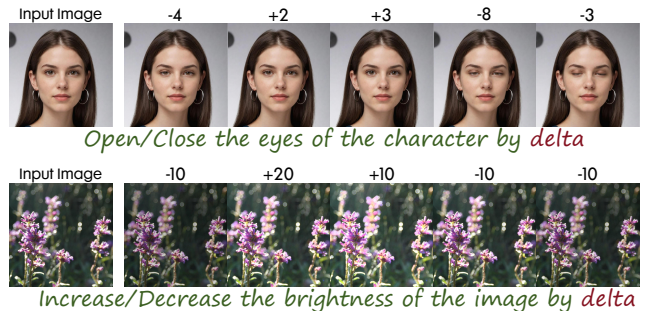


Figure 9. Visualization of Continuous Editing.

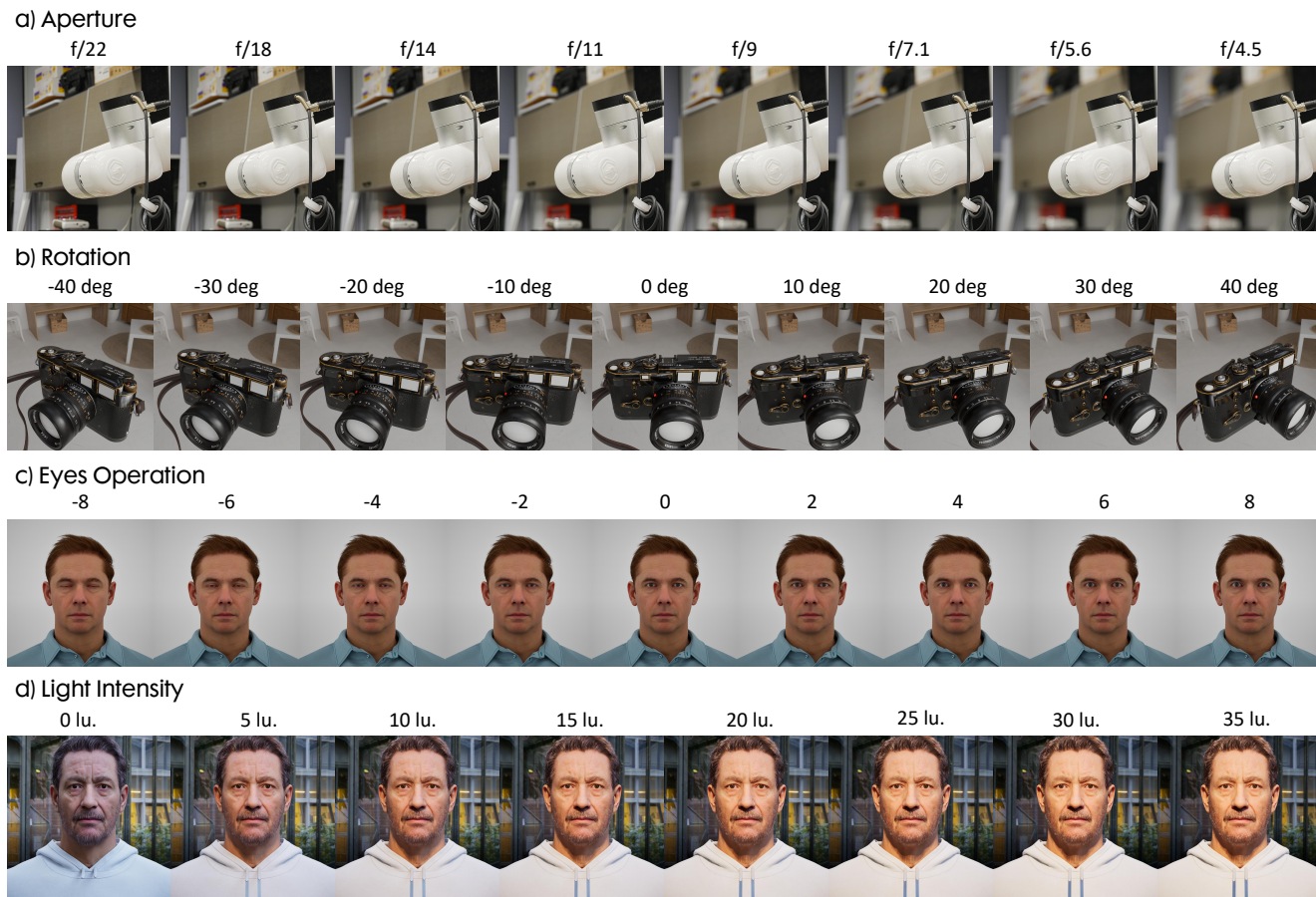


Figure 10. Visualization of samples in CAT dataset.

Fig.9, despite the first row’s cumulative parameter changes totaling  $-10$ , the final state exhibits incomplete closure; conversely, the second row achieves zero net change yet displays reduced brightness. While continuous editing cannot guarantee absolute numerical precision, the overall directional trends remain consistent.

## D. More Details on Synthesized Dataset

We illustrate samples from our Common Attribute Transformation dataset in Fig.10. All samples are annotated with accurate attribute values. For facial expression tasks such as eye opening (Fig.10 (c)), we use a simple gray HDRI for training. This choice does not interfere with the model’s generalization ability. However, for lighting-related tasks such as intensity adjustment (Fig.10(d)), we employ diverse HDRI backgrounds. This design reflects the complexity of real-world lighting conditions. Multiple HDRIs approximate these complex light sources and improve generalization performance. For object manipulation scenarios (Fig.10(b)), the object name is inserted into the instruction template. All low-level tasks follow a unified prompt for-

mat described in Sec.4.4, as shown in Fig.10 (a). All images in our dataset is taken in  $1024 \times 1024$ . During training, the samples are resized to  $512 \times 512$ .